Supplement of Eur. J. Mineral., 38, 53–73, 2026
https://doi.org/10.5194/ejm-38-53-2026-supplement

European Journal of Mineralogy
Open Access

Supplement of

Deciphering crystal growth in a sector-zoned interpenetration twin of loparite from Mt Khibiny (Kola Peninsula, Russia) through atomic-scale characterisation of growth sectors and twin boundaries

Nina Daneu et al.

Correspondence to: Nina Daneu (nina.daneu@ijs.si) and José Alberto Padrón-Navarta (alberto.padron@csic.es)

Supplementary materials

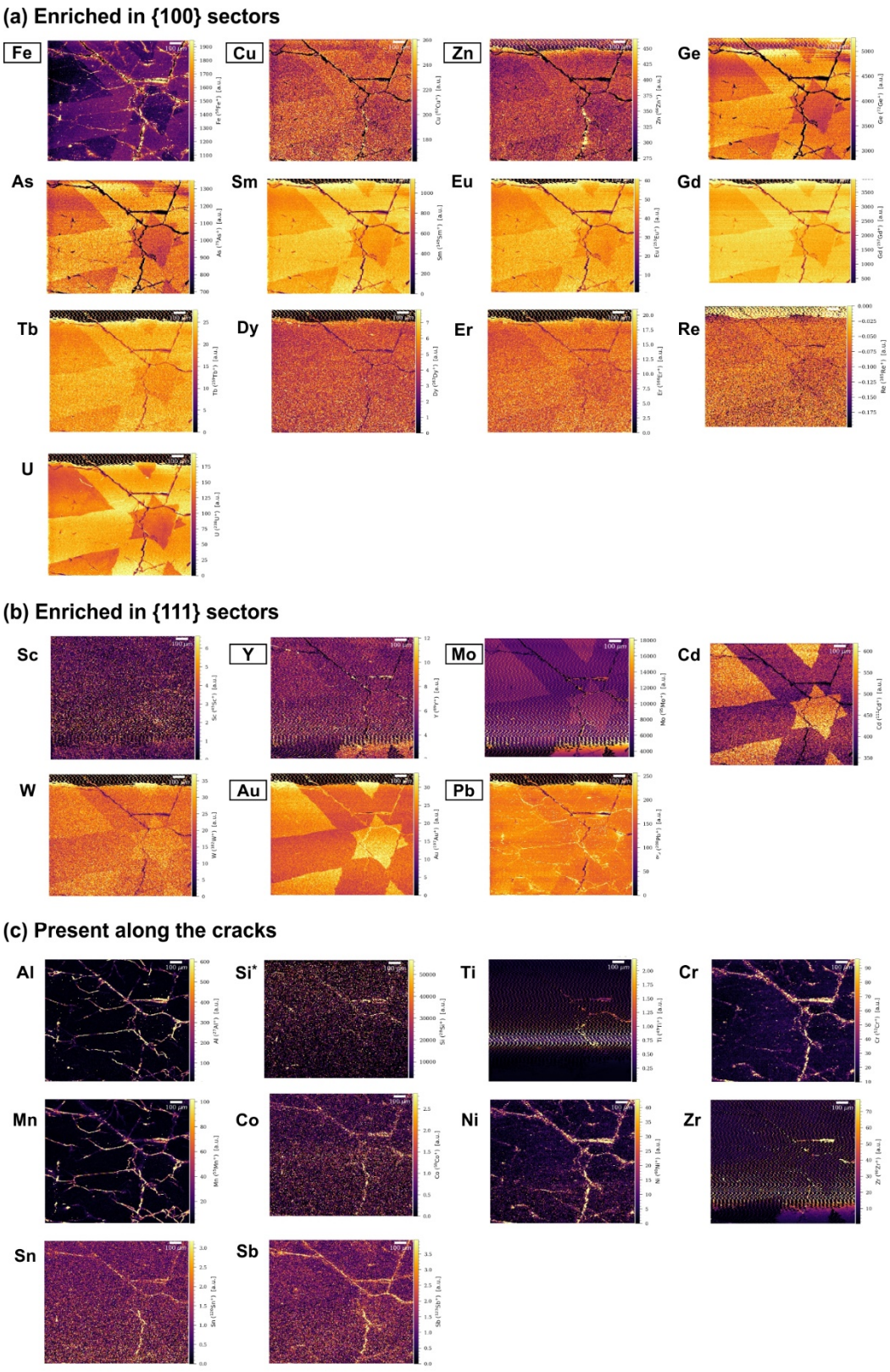

Figure S1: LA-ICP-TOF-MS elemental maps that reveal the presence of elements in minor/trace amounts. (a) Elements enriched in {100} sectors; (b) Elements enriched in {111} sectors. Elements in squares are present also in the cracks. (c) Elements detected only in the cracks. * Si was confirmed with STEM/EDX.

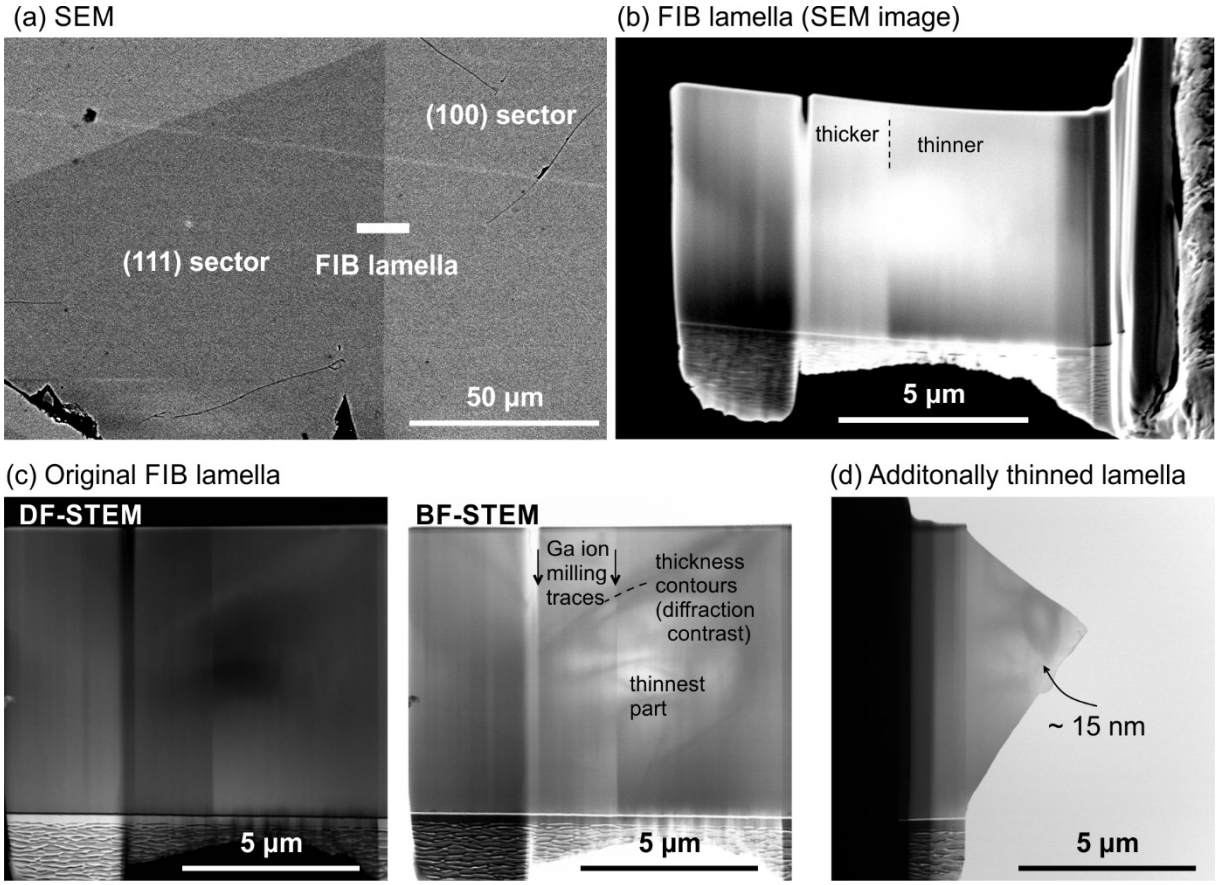

Figure S2: Preparation of FIB lamella across the sector boundary. (a) SEM image of the sector boundary and locality of the FIB lamella. (b) SEM image of the prepared lamella. (c) Low magnification DF-STEM and BF-STEM images of the lamella showing that the sector boundary is not visible. (d) BF-STEM image of the lamella after additional thinning to obtain regions thin enough (below 20 nm) for quantitative evaluation of the composition with HAADF-STEM in both growth sectors.

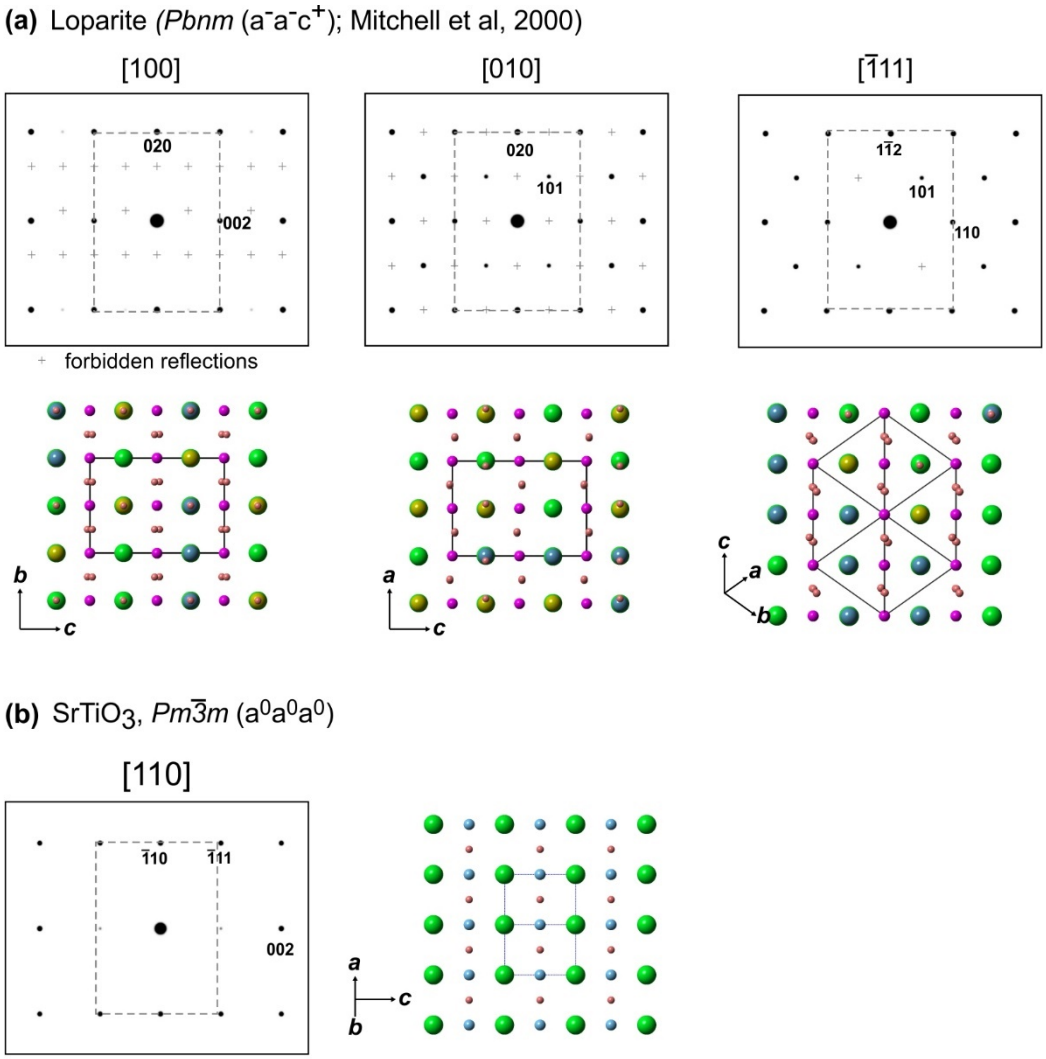

Figure S3: (a) Calculated diffraction patterns for orthorhombic loparite along the three [110] pseudocubic zone axes. and comparison with (b) diffraction pattern of cubic tausonite along the [110] zone axis. Structural models of both phases for the different orientations are also shown.

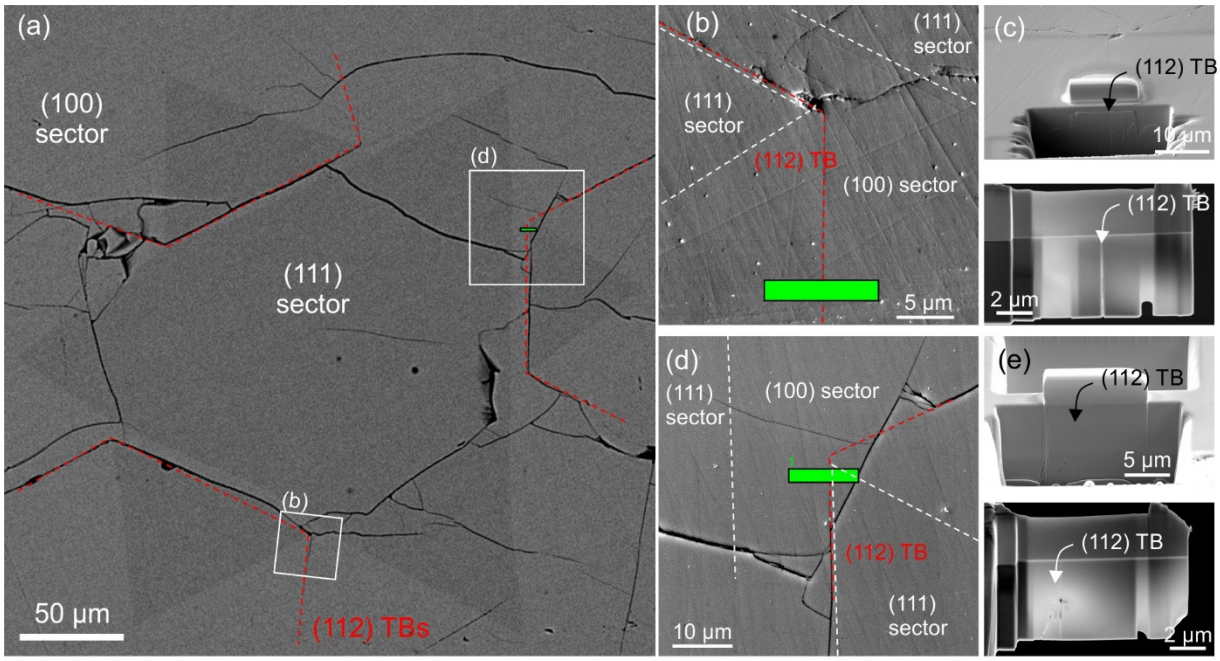

Figure S4: (a) Loparite cross-section along the [111] pseudocubic zone axis with marked locations for the preparation of FIB lamellae for analysis of {112} TB contacts. (b) Marked location (green square) of the FIB lamella for preparation of the edge-on oriented {112} TB. (c) This TB progresses vertically into the cross section (111) TB. (d) Location (green square) of the FIB lamella of the {112} TB contact that connects two edge-on {112}TBs. (e) This contact progresses into the interior of the crystal at an angle.

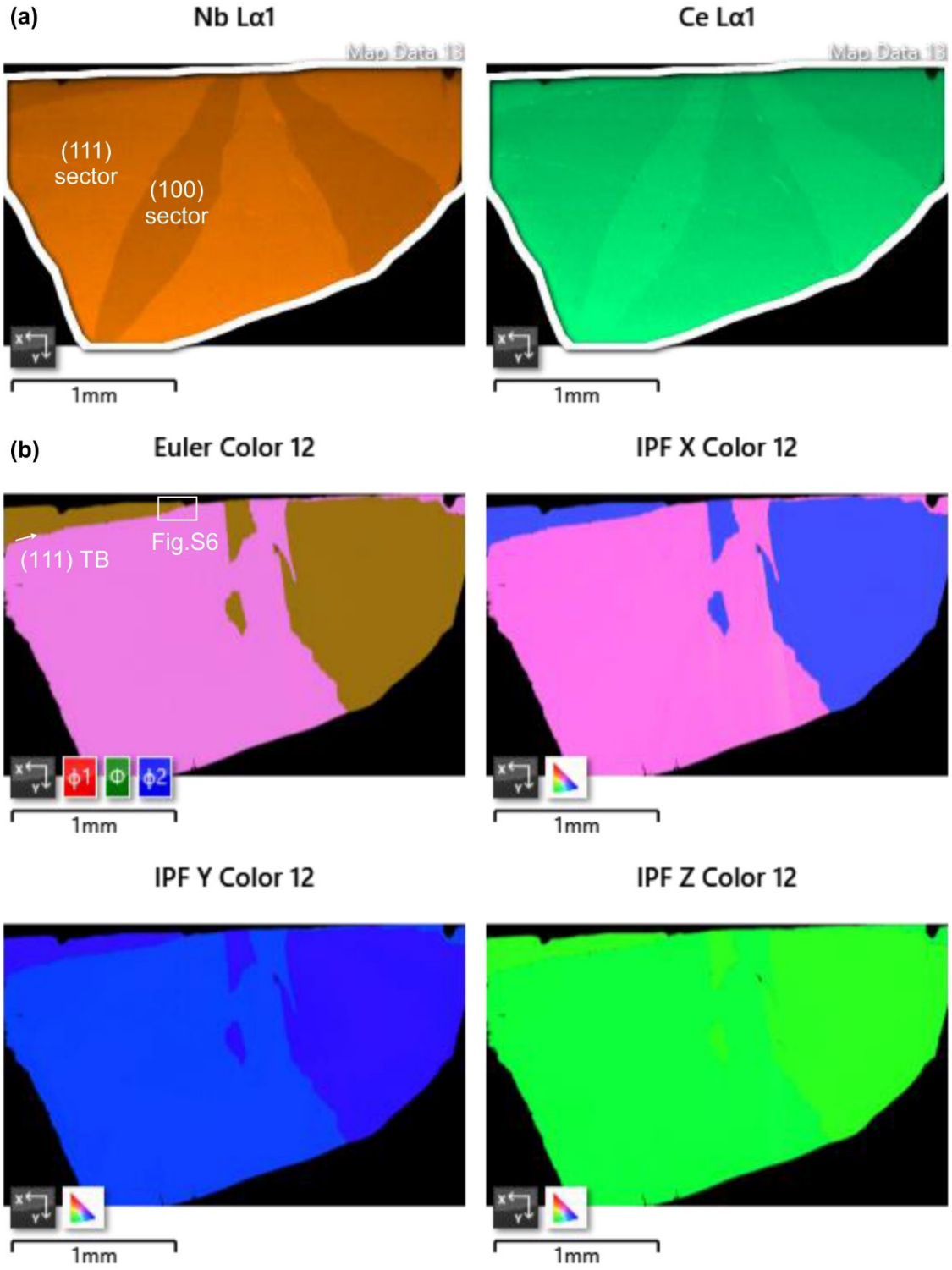

Figure S5: EDS-EBSD mapping of the cross-section perpendicular to the (111) TB. (a) Nb and Ce maps disclose the growth sectors. (b) EBSD mappings reveal the twin domains. The (111) TB progresses close to the edge of the sample, which is a cross-section along the [111] zone axis (see Fig. 2). The {112} TBs were sectioned at an angle, therefore a well-defined pattern is not observed.

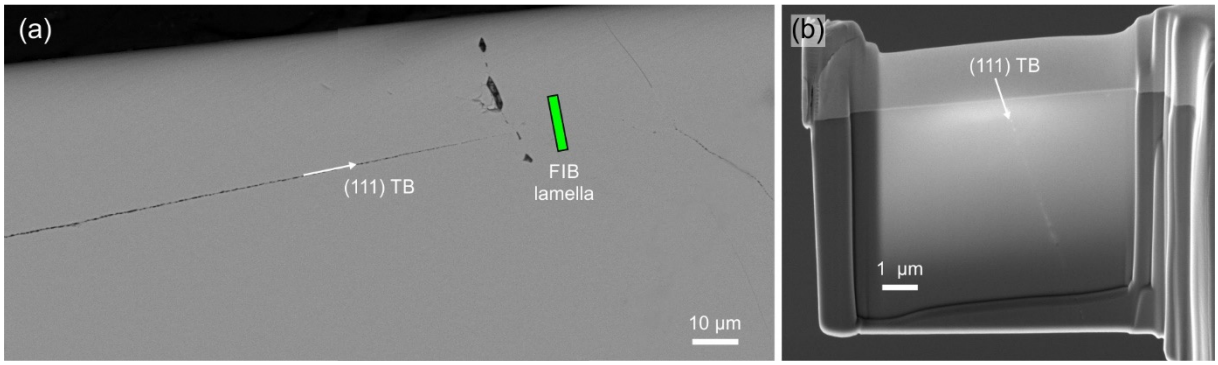

Figure S6: (a) Area, where the FIB lamella for the analysis of the (111) TB was prepared. The (111) TB is mostly porous contact, the FIB lamella was prepared across apparently tight contact between the domains. (b) FIB lamella with visible (111)TB. Inclination of the contact is due to the miscut of the crystal during the preparation.

Table S1: The results of EPMA in at%.

	DataSet/ Point	Na	Sr	Nb	Ti	La	Ce	Pr	Nd	Th	Fe	Ta	Ca	Si	O	Total
(100) TD2	1	11.198	0.6205	4.601	15.3157	2.0836	3.7178	0.2884	0.6516	0.0597	0.0395	0.127	1.164	0.0026	60.1307	100
	2	11.2111	0.6201	4.553	15.2835	2.1295	3.7168	0.3058	0.6509	0.0618	0.05	0.1294	1.1893	0.0028	60.0962	100
	3	11.0964	0.612	4.5605	15.3354	2.1269	3.743	0.2933	0.6626	0.0632	0.0473	0.1221	1.1707	0.0076	60.1592	100
	4	11.2477	0.5989	4.5646	15.3081	2.1178	3.7315	0.2719	0.6667	0.0612	0.049	0.1274	1.1547	-0.0003	60.1008	100
	5	11.1758	0.6136	4.5166	15.3567	2.1299	3.7515	0.2904	0.6609	0.0631	0.0403	0.1217	1.1648	0.0012	60.1135	100
	6	11.1988	0.6406	4.5002	15.3722	2.1188	3.7167	0.2997	0.6583	0.0606	0.0356	0.1296	1.1695	0.0022	60.0973	100
	7	11.1819	0.6083	4.4784	15.423	2.1044	3.7266	0.2859	0.6741	0.0657	0.0462	0.125	1.1612	0.0058	60.1136	100
	8	11.1829	0.6052	4.4337	15.4331	2.138	3.7626	0.2818	0.6711	0.0661	0.0522	0.1259	1.1466	0.0005	60.1003	100
	9	11.1646	0.6473	4.4071	15.4242	2.1448	3.7587	0.2989	0.6623	0.0691	0.0521	0.1358	1.1449	-0.0013	60.0913	100
	10	11.1456	0.6239	4.3619	15.4734	2.1173	3.8308	0.2903	0.6579	0.0676	0.0363	0.1311	1.1768	0.0001	60.087	100
	11	11.1525	0.616	4.3387	15.5605	2.1293	3.7939	0.2918	0.6775	0.0659	0.0409	0.1256	1.1047	-0.0028	60.1053	100
	12	11.1513	0.6067	4.3386	15.5552	2.1767	3.7537	0.2912	0.6627	0.0731	0.0485	0.1185	1.1262	-0.0032	60.1008	100
	13	11.269	0.6113	4.3831	15.475	2.1365	3.7645	0.3052	0.6501	0.0695	0.0426	0.113	1.1265	0.0012	60.0524	100
	14	11.1756	0.6094	4.3138	15.5307	2.153	3.7932	0.2908	0.6832	0.071	0.0383	0.1226	1.1358	0.0057	60.0768	100
	15	11.3683	0.594	4.2697	15.5645	2.1446	3.7368	0.3114	0.6761	0.0724	0.0354	0.1158	1.1169	0.0017	59.9924	100
(100) TD1	1	11.2409	0.6034	4.5775	15.2827	2.1127	3.737	0.2899	0.6359	0.0645	0.0474	0.1298	1.1707	0.0053	60.1023	100
	2	11.1533	0.6112	4.458	15.4013	2.1177	3.786	0.292	0.6524	0.0625	0.0506	0.1403	1.1632	-0.0036	60.1152	100
	3	11.1509	0.6172	4.3936	15.506	2.115	3.8104	0.2803	0.6451	0.0654	0.0395	0.1258	1.1364	0.0028	60.1116	100
	4	11.1137	0.6255	4.4578	15.4933	2.1328	3.7355	0.2878	0.6499	0.066	0.0338	0.1335	1.1124	0.0023	60.1558	100
	5	11.1639	0.6203	4.296	15.5608	2.1666	3.7799	0.2861	0.654	0.0682	0.0638	0.1228	1.1386	0.0025	60.0765	100
(111) TD2	1	11.4974	0.6907	5.4256	14.4624	1.9587	3.423	0.2603	0.58	0.0504	0.0398	0.1662	1.3014	0.0019	60.1423	100
	2	11.3954	0.6792	5.3781	14.5747	1.9656	3.4242	0.2664	0.5767	0.0461	0.0275	0.173	1.3023	0.0007	60.1903	100
	3	11.6028	0.6767	5.3943	14.4616	1.954	3.4144	0.2714	0.6011	0.0455	0.0443	0.1579	1.2834	0.0029	60.0897	100
	4	11.5433	0.6963	5.3851	14.4645	1.9744	3.441	0.2527	0.5881	0.0488	0.0513	0.161	1.2847	0.0009	60.1078	100
	5	11.4896	0.7075	5.3769	14.4961	1.9851	3.4473	0.2644	0.593	0.0488	0.0414	0.1495	1.2682	0.003	60.1291	100
	6	11.4278	0.6793	5.343	14.5942	1.9836	3.4382	0.2669	0.594	0.0439	0.0436	0.1564	1.2562	0.0031	60.1698	100
	7	11.3831	0.6735	5.3252	14.6125	2.0044	3.4418	0.2696	0.5838	0.042	0.0377	0.1591	1.2795	0.0058	60.182	100
	8	11.3663	0.6702	5.3145	14.6137	1.9934	3.4564	0.2728	0.5897	0.0501	0.0417	0.1562	1.2903	0.002	60.1828	100
	9	11.3913	0.6954	5.2868	14.6676	1.9833	3.4455	0.2649	0.5928	0.0499	0.0358	0.1514	1.2638	0.0009	60.1706	100
	10	11.4033	0.6758	5.2646	14.6229	2.0226	3.4674	0.276	0.5954	0.0495	0.0413	0.1498	1.2865	-0.0011	60.1462	100
	11	11.5171	0.6761	5.2126	14.629	2.0228	3.4811	0.2662	0.5861	0.0527	0.0492	0.1457	1.2823	-0.0018	60.0808	100
	12	11.4298	0.6937	5.231	14.6578	2.0096	3.4871	0.2664	0.5971	0.0515	0.0401	0.1463	1.2605	-0.0007	60.1299	100
	13	11.4239	0.6799	5.2106	14.7108	2.0005	3.4594	0.2794	0.6003	0.0483	0.0361	0.1516	1.2536	0.0042	60.1413	100
	14	11.4003	0.6605	5.1676	14.6977	2.032	3.5377	0.2685	0.5996	0.0546	0.0292	0.1542	1.2601	0.0026	60.1354	100
	15	11.4752	0.6861	5.1852	14.6951	2.0329	3.4775	0.276	0.5877	0.0553	0.0371	0.157	1.219	-0.0001	60.1159	100
(111) TD2	1	11.4121	0.678	5.3982	14.5298	1.9592	3.3905	0.2535	0.6011	0.0442	0.0614	0.1625	1.331	0.005	60.1734	100
	2	11.4021	0.6872	5.4165	14.5152	1.9653	3.4042	0.2688	0.5734	0.051	0.0346	0.1702	1.3275	-0.0002	60.1841	100
	3	11.5085	0.6831	5.4391	14.45	1.9785	3.4025	0.2797	0.5882	0.0426	0.0296	0.1599	1.2993	0.0005	60.1384	100

Table S2: Composition of the A- and B-sites for preparation of models for image simulations of the (100) sector (Model '100'). The values represent fractions of the element on the A- or B-sites. The elements were randomly distributed to the A- and B-sites.

	A-sites								B-sites			
	Na	Ce	La	Nd	Pr	Ca	Sr	**Σ A**	Ti	Nb	Ta	**Σ B**
A	0.566	0.188	0.105	0.033	0.015	0.059	0.031	**0.997**	0.772	0.222	0.006	**0.998**

Table S3: (a) Average chemical composition of the {111} sector according to EPMA. Distribution of light (Na) an heavy (LREE) elements to the A1 and A2 sites in different ratios. The occupancies are given in at% and recalculated to obtain full occupancy of atomic columns (ΣA and ΣB close to 1).

		A-sites										B-sites			
(a)		Na	Ce	La	Nd	Pr	LREE	Ca	Sr	Ca+Sr	Σ A	Ti	Nb	Ta	Σ B
EPMA {111} sector	A	0.582	0.173	0.099	0.029	0.013	0.314	0.066	0.035	0.101	0.997	0.720	0.270	0.008	0.998
(b)			Na					LREE			Ca+Sr				
			A1:A2					A1:A2			A1:A2				
Model '111-1'	A1	0.518	45:55	0.208	0.119	0.035	0.016	60:40	0.066	0.035	50:50	0.997	0.720	0.270	0.008	0.998
	A2	0.646		0.138	0.079	0.023	0.010		0.066	0.035		0.997				
Model '111-2'	A1	0.452	39:61	0.244	0.141	0.042	0.017	70:30	0.066	0.035	50:50	1.000	0.720	0.270	0.008	0.998
	A2	0.706		0.104	0.061	0.018	0.008		0.066	0.035		0.998				
Model '111-3'	A1	0.454	34:66	0.242	0.139	0.041	0.018	80:20	0.066	0.035	50:50	0.995	0.720	0.270	0.008	0.998
	A2	0.710		0.104	0.059	0.017	0.008		0.066	0.035		0.995				

Table S4: Quantitative analysis of high-resolution HAADF-STEM image of the (111) sector, image simulations of model with random distribution of elements as given in Table 4. Correlation analysis shows best match between the simulation of the model with 19.7 nm thickness and experimental image with thickness of around 17 nm as determined by EELS analysis.

		Quantitative analysis of experimental and simulated images										Correlation analysis (Fig. 7b)							
			A1 sites		A2 sites		B sites		Intensity ratios			Correlation Coefficients (Sim:Exp)						Avr CorrCoef Exp:Sim	StDev CorrCoef Exp:Sim
		Thickness	AbsInt A1	StDev A1	AvrInt A2	StDev A2	AvrInt B	StDev B	A1:B	A2:B	A1:A2								
		nm	counts	in %	counts	in %	counts	in %				A1 StDev	A2 StDev	B StDev	A1:B	A2:B	A1:A2		
(a) Experimental (Exp, Fig. 7a)		**~17***	3601	**14.1**	2847	**16.2**	2730	**8.5**	**1.3**	**1.0**	**1.3**								
(b) Simulations (Sim)	**Model '111-1'**	4.8	4.37	39.2	2.9	52.3	3.0	19.4	1.5	1.0	1.5	2.8	3.2	2.3	1.1	0.9	1.2	1.92	0.97
	A1:A2	9.8	7.83	24.4	5.2	33.2	5.4	13.6	1.4	0.9	1.5	1.7	2.0	1.6	1.1	0.9	1.2	1.43	0.43
	Na: 45:55	**19.7**	12.6	**10.8**	9.3	**16.2**	10.0	**6.5**	**1.3**	**0.9**	**1.4**	**0.8**	**1.0**	**0.8**	**1.0**	**0.9**	**1.1**	**0.91**	**0.12**
	Sr. Ca: 50:50	29.6	15.3	10.2	13.0	8.9	13.6	4.7	1.1	1.0	1.2	0.7	0.5	0.6	0.9	0.9	0.9	0.75	0.17
	LREE: 60:40	59.5	22.2	5.2	20.4	4.2	22.0	1.9	1.0	0.9	1.1	0.4	0.3	0.2	0.8	0.9	0.9	0.56	0.31
	Model '111-2'	4.8	5.2	39.4	3.0	42.7	3.2	23.6	1.6	0.9	1.7	2.8	2.6	2.8	1.2	0.9	1.4	1.94	0.87
	A1:A2	9.8	9.1	24.4	5.0	28.0	5.6	13.4	1.6	0.9	1.8	1.7	1.7	1.6	1.2	0.9	1.4	1.43	0.33
	Na: 39:61	**19.7**	13.5	**12.0**	8.8	**15.9**	9.9	**7.0**	**1.4**	**0.9**	**1.5**	**0.8**	**1.0**	**0.8**	**1.0**	**0.9**	**1.2**	**0.96**	**0.15**
	Sr. Ca: 50:50	29.6	16.8	7.7	11.4	10.0	13.6	4.8	1.2	0.8	1.5	0.5	0.6	0.6	0.9	0.8	1.2	0.77	0.24
	LREE: 70:30	59.5	23.6	4.9	19.2	5.3	21.8	1.8	1.1	0.9	1.2	0.3	0.3	0.2	0.8	0.8	1.0	0.59	0.33
	Model '111-3'	4.8	5.4	28.3	2.2	54.5	3.2	23.7	1.7	0.7	2.5	2.0	3.4	2.8	1.3	0.7	2.0	2.02	0.97
	A1:A2	9.8	9.9	14.0	3.4	31.3	5.6	12.4	1.8	0.6	2.9	1.1	1.9	1.5	1.3	0.6	2.3	1.45	0.62
	Na: 34:66	**19.7**	14.6	**9.2**	6.7	**15.2**	9.8	**8.5**	**1.5**	**0.7**	**2.2**	**0.7**	**0.9**	**1.0**	**1.1**	**0.7**	**1.7**	**1.02**	**0.39**
	Sr. Ca: 50:50	29.6	18.1	6.2	10.3	11.3	13.7	5.0	1.3	0.7	1.8	0.4	0.7	0.6	1.0	0.7	1.4	0.81	0.34
	LREE: 80:20	59.5	24.4	5.1	18.1	5.9	21.9	2.2	1.1	0.8	1.3	0.4	0.4	0.3	0.8	0.8	1.1	0.61	0.33

* Determined from EELS

Text S1: Calculation of the correlation between experimental images and image simulations

Loparite exhibits complex chemical composition with a mixture of high-Z and low-Z elements on the A- and B-sites. In the crystal we investigated, the A- and B-site elements are randomly distributed to the two types of atomic columns in the (100) sector, whereas the A-site elements show a certain degree of ordering in the (111) sector to the A1 and A2 sites. Chemical composition of single atomic columns varies arbitrarily, which reflects in the variable intensity of the atomic columns and prevents direct comparison (Van Aert et al., 2009) of the experimental and simulated images.

For this reason, we used an alternative (indirect) approach for evaluation of the correlation between simulated images and the experimental image. We compared relative standard deviations (RelStDev) of the atomic columns intensities, separately for all atomic column types in every sector. For the (100) sector, we used standard deviations of the A and B columns and A:B intensities ratio, and for the (111) sector, we used relative standard deviations of the A1, A2 and B columns and A1:B, A2:B and A1:A1 intensity ratios. Average correlation coefficients and their standard deviations were calculated as:

$$\mathrm{Avg}_{\mathrm{CorrCoef}} = \frac{1}{\mathrm{n}}\sum_{\mathrm{i}=1}^{\mathrm{n}} r_i$$

$$\mathrm{StDev}_{\mathrm{CorrCoef}} = \sqrt{\frac{1}{\mathrm{n}-1}\sum_{\mathrm{i}=1}^{\mathrm{n}} (r_i - \bar{r})^2}$$

Cubic sector: n = 3; i = A, B and A:B

Octahedral sector: n=6; i = A1, A2, B, A1:B, A2:B and A1:A2

The simulated image that has $\mathrm{Avr}_{\mathrm{CorrCoef}}$ closest to unity and lower $\mathrm{StDev}_{\mathrm{CorrCoef}}$ is considered as the best match between the simulated and experimental image – model with most similar thickness and composition.

The starting models were prepared based on the results of the chemical analysis of the growth sectors with EPMA, whereas the thickness of the sample in the experimental image was estimated by EELS.